JACS
JOURNAL OF THE AMERICAN CHEMICAL SOCIETY
Article
pubs.acs.org/JACS

Structural Organization of Insulin Fibrils Based on Polarized Raman Spectroscopy: Evaluation of Existing Models

Valentin Sereda,[†] Michael R. Sawaya,[‡] and Igor K. Lednev*[,†]

[†]Department of Chemistry, University at Albany, SUNY, 1400 Washington Avenue, Albany, New York 12222, United States
[‡]UCLA–DOE Institute, 611 Charles E. Young Drive, Los Angeles, California 90095-1570, United States

Supporting Information

ABSTRACT: Many different proteins undergo misfolding and self-assemble into amyloid fibrils, resulting in a range of neurodegenerative diseases. The limitations of conventional methods of structural biology for fibril characterization have led to the use of polarized Raman spectroscopy for obtaining quantitative structural information regarding the organization of amyloid fibrils. Herein, we report the orientation of selected chemical groups and secondary structure elements in aligned insulin fibrils, including β-sheets, which possess a high level of orientation in the cross-β core, and α-helices in the disordered portions of the fibrils. Strong orientation of disulfide bonds in amyloid fibrils was also revealed, indicating their association with the fibril core. The determined orientation of chemical groups provides strong constraints for modeling the overall structure of amyloid fibrils, including the core and disordered parts. The developed methodology allows for the validation of structural models proposed in the literature for amyloid fibrils. Specifically, the polarized Raman data obtained herein strongly agreed with two insulin fibril models (Jiménez et al., *Proc. Natl. Acad. Sci. U. S. A.* **2002**, *99*, 9196–9201 and Ivanova et al., *Proc. Natl. Acad. Sci. U. S. A.* **2009**, *106*, 18990–18995) yet revealed significant qualitative and quantitative differences. This work demonstrates the great potential of polarized Raman spectroscopy for structural characterization of anisotropic biological species.

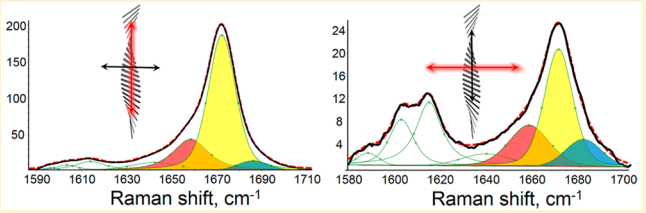

INTRODUCTION

Amyloid aggregation, a specific form of protein misfolding and self-assembly, has been associated with several human diseases, including Parkinson's disease, Alzheimer's disease, and type II diabetes.[1−3] Despite considerable diversity in the amino acid sequence of the precursor proteins, amyloid fibrils share a number of common structural features. Amyloid fibrils are typically long, unbranched entities[4,5] with the classic "cross-β" structure in which individual strands in the β-sheets are aligned perpendicular to the long axis of the fibril.[6,7] To date, the majority of structural information about amyloid fibrils has come from solid-state NMR,[8] cryo-EM,[9] single-crystal X-ray diffraction analysis,[7,10] electron paramagnetic resonance,[11] X-ray and electron fiber diffraction, and scanning probe microscopy.[1,5] Structural information for a number of amyloidogenic peptides has also been obtained by means of infrared linear dichroism spectroscopy,[12−14] deep UV resonance Raman spectroscopy,[15] infrared spectroscopy,[13,16,17] and vibrational circular dichroism.[4,18] The vast majority of these techniques and methods report on the fibril core structure, whereas the organization of the remainder of the fibril aggregate remains elusive. Recent tip enhanced Raman (TER) spectroscopic studies have shown significant presence of α-helical and unordered protein on the fibril surface.[19,20] Several detailed structural models have been reported for amyloid fibrils,[21−23] including those formed from human insulin.[24−26] The models are typically based on a relatively accurate structure determination of the core with much less information on the other parts of the fibril. One of the main goals of this study is to verify the fibril structural models based on polarized Raman spectroscopy of aligned fibrils.

Raman spectroscopy is a powerful nondestructive technique for the structural characterization of proteins and protein aggregates.[27] Its advantages include high sensitivity to changes in conformation and chemical bonding. Moreover, the orientation of individual structural units in the sample can be evaluated on the basis of polarized Raman measurements conducted on an anisotropic sample of aligned species. Polarization characteristics of Raman scattering are related to the polarizability tensor and contain information regarding the symmetry of chemical groups. Raman band anisotropy measurements allow for retrieval of this information if the Raman tensor is known.[28−37] Polarized infrared absorption and Raman spectroscopies have been utilized for studying amyloid fibrils. In particular, the orientation of the β-strands, tyrosine and phenyl rings relative to the fibril axis has been demonstrated.[13,14,38] Additionally, inclination angles for specific C═O bonds with respect to the fibril axis of amyloid fibrils, prepared from the core fragment (21−31 peptide, [^{21}NFLNCYVSGFH^{31}]) of β_2-microglobulin, have been reported.[12,39]

Received: April 29, 2015
Revised: July 19, 2015
Published: August 15, 2015

DOI: 10.1021/jacs.5b07535
J. Am. Chem. Soc. 2015, 137, 11312−11320

The theoretical background of orientation measurements by Raman spectroscopy has been extensively described in the literature devoted to polarized Raman spectroscopic measurements,[32] and the general procedure for determining the order parameters $\langle P_2 \rangle$ and $\langle P_4 \rangle$ has been developed in detail by Bower.[31] Only the second ($\langle P_2 \rangle$) and fourth ($\langle P_4 \rangle$) coefficients of the orientation function can be determined with polarized Raman spectroscopy, from which the orientation distribution can be estimated by calculating the most probable orientation function, $N_{mp}(\theta)$.[33,40−42]

A number of alignment techniques have been used for the molecular orientation of fibrils, including methods utilizing stretched polyethylene films as a matrix,[36] shear flow orientation of macromolecules,[43,44] molecular combing,[13,38,45] and preparation of dried stalk samples.[38,45] Among these approaches, the method based on drop coating deposition Raman (DCDR) spectroscopy[46−48] has been used with polarized Raman spectroscopy to obtain structural information on oriented amyloid fibrils.

In this work, we utilized polarized Raman spectroscopy of aligned insulin fibrils to determine the orientation of individual secondary structural elements, including β-sheets, α-helices and "disordered" parts of the protein backbone as well as two interchain disulfide bonds. Two structural models for complete human insulin fibrils, which have been reported previously,[24,25] were evaluated on the basis of the results reported herein.

RESULTS AND DISCUSSION

Polarized Raman Spectra of Aligned Fibrils. Polarized Raman spectroscopy was utilized in this work for probing the molecular organization of insulin fibrils. To determine the orientation of specific chemical groups, anisotropic samples of aligned fibrils were prepared using the drop coating deposition method.[46−48] Briefly, approximately 20 μL of fibril suspension was deposited onto aluminum foil and allowed to dry. It has been shown that this simple method is extremely efficient and results in a high degree of fibril alignment.[49]

Raman spectra were acquired using four polarization geometries (XX, ZZ, XZ, and ZX), where the first and second letters correspond to the incident and scattered light polarizations, respectively (Figure 1, Inset). The laboratory coordinate system (XYZ) is defined in such a way that the Z-axis corresponds to the main axis of the aligned fibrils and the Y-axis corresponds to the propagation direction of the incident and scattered (collected) light.

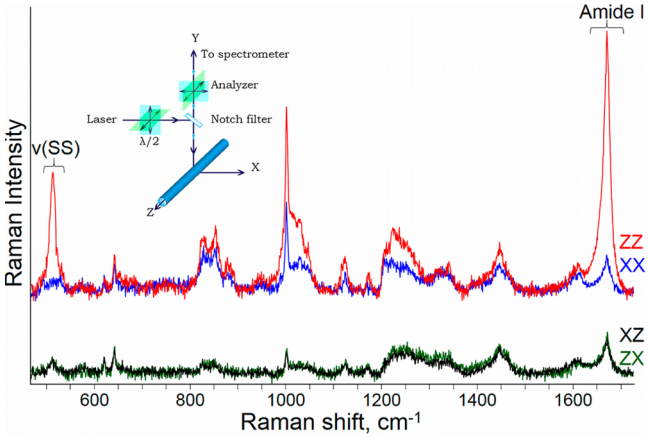

Figure 1. Normalized polarized Raman spectra of oriented human insulin fibrils.

Significant differences in intensity were observed for several vibrational modes in the Raman spectra acquired using the XX and ZZ polarization geometries. In particular, the bands in the 1575−1720 cm^{-1} and 480−550 cm^{-1} regions, corresponding to the amide I[50,51] and disulfide stretching modes,[52] respectively, exhibited major variations. To obtain qualitative information regarding the degree of alignment, we calculated the orientation parameter f, also termed the pseudo-order parameter, using the following formula:[53]

$$f = 1 - (I_{XX}/I_{ZZ})$$

where I_{XX} and I_{ZZ} are the Raman intensities of the peak of interest in the XX and ZZ spectra, respectively. For an isotropic sample, f equals zero and increases as the molecular orientation increases along the Z direction until it reaches 1 for a perfect parallel orientation. We obtained f values of 0.88 and 0.91 for the 1672 cm^{-1} amide I band and 513 cm^{-1} S−S stretching vibration band, respectively.

Amide I Vibrational Mode. The amide I Raman band is mainly associated with the C═O stretching mode, with additional contributions from C−N stretching and Cα−C−N deformation.[54−57] It has been shown previously[50,58,59] that Raman spectra of amyloid fibrils in general, and the amide I band in particular, are dominated by the contribution from the fibril core, which has a well-ordered β-sheet structure with β-strands arranged parallel or antiparallel to each other and perpendicular to the long axis of the fibril.[13,60] Consequently, because of the cross-β structure of the fibril core, peptide carbonyl groups are oriented nearly parallel to the main axis of the fibril.[13,14,38] Specifically, the peptide carbonyl group angle of 13 ± 5° relative to the fibril axis has been reported for insulin fibrils.[49] Hiramatsu et al.[12,39] determined the orientation of various C═O groups in fibrils prepared from the core fragment (21−31 peptide) of β_2-microglobulin (0° angle for two C═O bonds and 27° angle for three C═O bonds in the β-sheet region of fibrils). In addition, there is a 47° angle for the four C═O groups in the random coil portion and a 32° angle for the two C═O groups in the β-turn or β-bulge portions.

It is currently well accepted that the fibril cross-β core is surrounded by randomly oriented protein regions with various secondary structures, including α-helices, β-turns, and disordered conformations.[19,61−63] Using tip-enhanced Raman spectroscopy, we have recently found that the secondary structure configuration and the amino acid residue composition are different on the surface of two insulin fibril polymorphs.[64]

The amide I normal vibrational mode depends on the C═O hydrogen bonding, on the vibrational coupling between adjacent amide units, and, consequently, on the protein secondary structure.[51,65,66] Therefore, the decomposition of the amide I Raman band on individual components allows for the determination of the protein secondary structure composition. The amide I region (1575−1720 cm^{-1}) of the polarized Raman spectra was fitted using Gaussian and Lorentzian functions, including three components representing the main secondary structural elements.[50] Figure 2 shows the band decomposition for the four polarized spectra with different polarization geometries. The component at 1672 cm^{-1} is assigned to the well-ordered β-sheet structure, whereas the band at ca. 1655 cm^{-1} is attributed to the α-helical conformation. The component at approximately 1685 cm^{-1} could reflect a composite contribution from PPII, a disordered

DOI: 10.1021/jacs.5b07535
J. Am. Chem. Soc. 2015, 137, 11312−11320

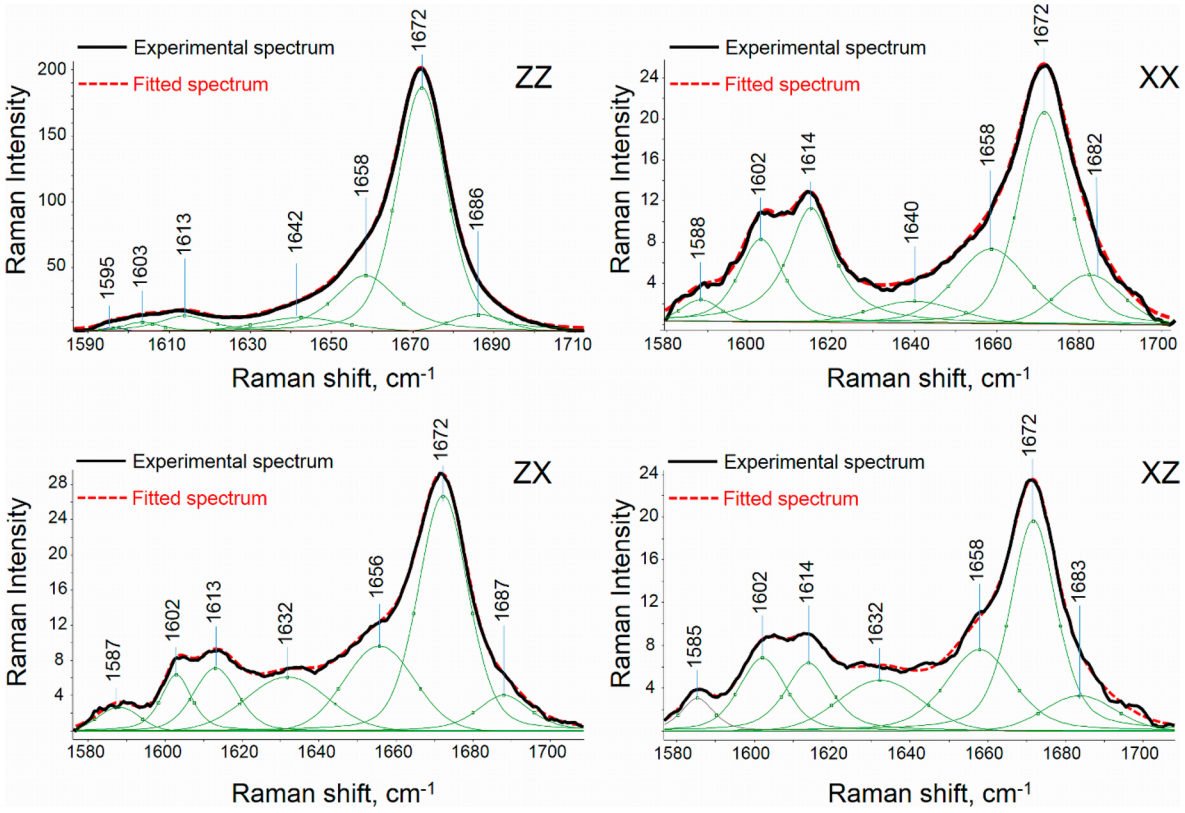

Figure 2. Band decomposition of the amide I region of the polarized Raman spectra of insulin fibrils for various polarization geometries.

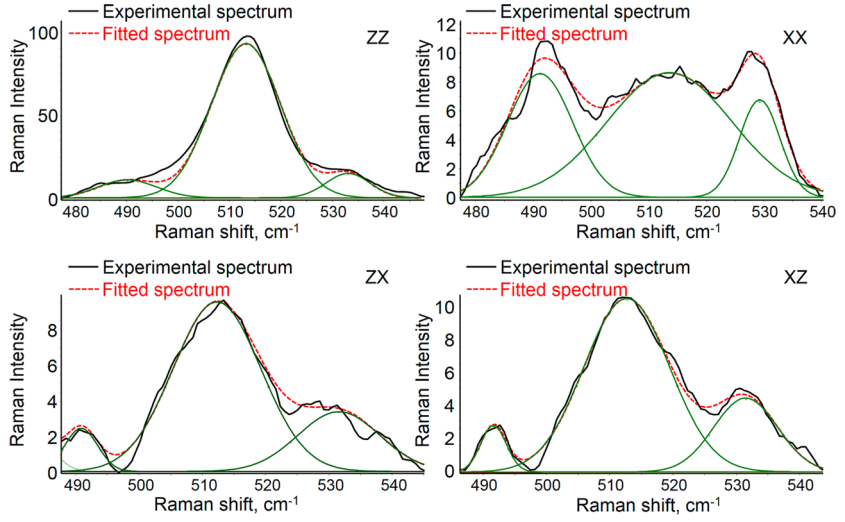

Figure 3. Band decomposition of the S−S stretching vibrational mode region of the polarized Raman spectra of oriented insulin fibrils for various polarization geometries.

structure. The bands at 1589, 1604, and 1616 cm^{-1}, which could be attributed to ring modes of Phe and Tyr residues,[67,68] were also included in the band-fitting protocol.

S−S Stretching Vibration. Protein Raman bands at 510 ± 5, 525 ± 5, and 540 ± 5 cm^{-1} could be assigned to S−S stretching vibrations, ν(SS), in gauche−gauche−gauche (*ggg*), gauche−gauche−trans (*ggt*) and trans−gauche−trans (*tgt*) conformations of the C−C−S−S−C−C segment, respectively.[69−72] Gaussian deconvolution of the Raman spectra of naive insulin and isotropic insulin fibril powders in the 470−580 cm^{-1} range revealed that the ratio between the peak areas assigned to the *ggg* and *ggt* conformations was approximately 2:1. Therefore, two out of the three disulfides most likely contribute to the 513 cm^{-1} Raman band, whereas the remaining S−S bond is responsible for the 530 cm^{-1} band. The positions of the disulfide bands in the Raman spectrum of native insulin powder were in agreement with the literature data.[46,68] The Raman peaks at approximately 490 cm^{-1} found in the spectra of native insulin and isotropic insulin fibril powders can be assigned to skeletal bending.[68] On the basis of the crystal structure of human insulin,[73] we assigned the most intense peak at 513 cm^{-1} (S−S) to two disulfides ([B] Cys7-[A] Cys7 and [B] Cys19-[A] Cys20) with a *ggg* conformation, whereas the

DOI: 10.1021/jacs.5b07535
J. Am. Chem. Soc. 2015, 137, 11312−11320

Table 1. Calculated Intensity Ratios R_z and R_x, Order Parameters $\langle P_2 \rangle$ and $\langle P_4 \rangle$, and Lagrange Multipliers λ_2 and λ_4 for Amide I and ν(SS) Raman Tensors in Human Insulin Fibrils

Raman shift, cm^{-1}	R_z	R_x	$\langle P_2 \rangle$	$\langle P_4 \rangle$	λ_2	λ_4	R_{iso}	a
1672 (β-sheet)	0.11	1.12	0.65	0.43	2.1	1.52	0.47	−0.115
1655 (α-helix)	0.19	1.23	0.51	0.22	2.09	0.43	0.49	−0.131
1685 (PPII, disordered structure)	0.22	1.38	0.5	0.2	2.11	0.31	0.45	−0.172
513 ν(SS)	0.1	1.23	0.69	0.46	2.3	1.6	0.47	−0.115

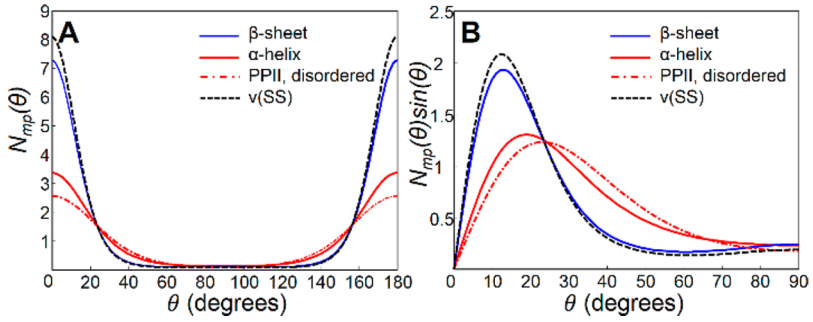

Figure 4. (A) The most probable orientation distribution function $N_{mp}(\theta)$ and (B) the calculated orientation distribution function $N_{mp}(\theta)\sin(\theta)$ of Raman tensors obtained for amide I Raman spectroscopic components and a disulfide Raman band of human insulin fibrils.

530 cm^{-1} peak was attributed to the disulfide bond ([A] Cys11-[A] Cys6) with a *ggt* conformation.

It is known that S−S stretching Raman bands have a very low depolarization coefficient, and the Raman tensor for the totally symmetric stretching vibration of the disulfide bridge is oriented parallel to the S−S bond.[74,75] As shown in Figure 3, the intensity of the band at 513 cm^{-1} is very strong in the ZZ orientation and weak in the XX orientation, indicating a high level of orientation of the disulfide bonds with a *ggg* conformation along the main axis of the insulin fibrils. To the best of our knowledge, this is the first experimental observation of a preferential orientation of disulfide bonds in amyloid fibrils.

Aromatic Amino Acid Residue Side Chains. The bands at 643, 830, and 1209 cm^{-1}, which could be assigned to various vibrational modes of the phenoxyl ring, and the bands at 1003 and 1032 cm^{-1}, which arise from phenylalanine residues, also showed different Raman scattering intensity for XX and ZZ configurations (Figure 1). It is well-known that aromatic residues play an important role in the stability of protein structures through the involvement of hydrogen bonds or in the stabilization of amyloid fibrils as a result of $\pi-\pi$ stacking between aromatic residues.[76] In addition, the Raman bands at approximately 830−850 cm^{-1} can be useful in determining the local environment of the Tyr side chains. It has been shown previously that the intensity ratio I_{850}/I_{830} depends strongly on the hydrogen-bonding state of the phenoxyl group.[77]

Orientation of Chemical Groups in Insulin Fibrils. Quantitative interpretation of polarized Raman spectra (Figure 1) requires the Raman tensor of a particular band. In general, a Raman tensor relates the polarization direction of the exciting light to the polarization direction of the scattered light.[28,78] A Raman tensor corresponding to a particular vibrational mode can be described in terms of three nonzero components (principal axes) that can be determined using polarized Raman spectroscopic measurements.[79] The procedure for determining the orientation of chemical groups based on polarized Raman spectroscopy has been previously reported.[35,80,81] Briefly, this method is based on acquiring four polarized Raman spectra (I_{ZZ}, I_{ZX}, I_{XX}, and I_{XZ}) in the backscattering configuration[35] (see the Supporting Information).

The polarized Raman spectra of oriented fibrils are depicted in Figure 1. Significant intensity variations are evident for several bands in the ZZ and XX spectra. The fact that the crossed-polarized spectra (ZX and XZ) overlap within the experimental error confirms that no displacements and rotations of the sample occurred during the measurements. Most importantly, this result satisfies the conditions for the application of the uniaxial model, which allows for quantitative determination of the order parameters $\langle P_2 \rangle$ and $\langle P_4 \rangle$ from the polarized Raman spectra.

The intensity ratios, $R_z = I_{ZX}/I_{ZZ}$ and $R_x = I_{XZ}/I_{XX}$, of the amide I band components and ν(SS), together with the corresponding values of the order parameters $\langle P_2 \rangle$ and $\langle P_4 \rangle$, are summarized in Table 1.

A positive $\langle P_2 \rangle$ value indicates that PART is preferentially oriented parallel to the fibril axis. In the case of the amide I band, this result is in agreement with the data previously reported for aligned amyloid fibrils studied by polarized infrared and Raman spectroscopies.[13,14,38]

We calculated the most probable orientation distribution function, $N_{mp}(\theta)$, based on experimentally determined $\langle P_2 \rangle$ and $\langle P_4 \rangle$ values and numerically calculated Lagrangian multipliers (λ_2 and λ_4) using a well-developed approach for quantitative characterization of Raman tensor orientation,[33,40−42] where θ is the angle between the fibril axis and the principal axis of the polarizability tensor. Because a uniaxial cylindrical symmetry was assumed, multiplication of the most probable orientation distribution function by $\sin(\theta)$ allows for the preferred orientation with respect to the fibril axis to be obtained, which corresponds to the maximum $N_{mp}(\theta)\sin(\theta)$ function (Figure 4). The mean of this distribution function characterizes the average orientation angle.[82,83]

Orientations of C═O Groups and Secondary Structure Elements. Figure 4A shows $N_{mp}(\theta)$ associated with various secondary structure components of the amide I band. In each case, $N_{mp}(\theta)$ is Gaussian, unimodal, and centered at θ = 0°. Thus, it can be concluded that different structural components are not randomly oriented but exhibit a certain level of orientation. As expected, the β-sheet component (1672 cm^{-1}) showed the highest level of orientation among all the

DOI: 10.1021/jacs.5b07535
J. Am. Chem. Soc. 2015, 137, 11312−11320

secondary structure elements. The distribution of orientation was broader for the α-helix (1655 cm^{-1}) and PPII/disordered structure (1685 cm^{-1}) than for the β-sheet. The $N_{mp}(\theta)\sin(\theta)$ function of the 1672 cm^{-1} band reached a maximum at $\theta = 12°$ with an average orientation angle of approximately 26°(Figure 4B). For the other two components of the amide I region, representing α-helices (ca. 1655 cm^{-1}) and composite contributions from PPII and disordered regions (near 1685 cm^{-1}), the average orientation angles of PART were 33° and 35°, respectively.

The ultimate goal of the polarized Raman spectroscopic study is to determine the orientation of chemical groups in an amyloid fibril based on the orientation distribution functions obtained for the polarizability tensors. The knowledge of the orientation of the polarizability tensor relative to the corresponding chemical group is required for this determination. The largest polarizability oscillation for the amide I vibration of the isolated amide chromophore occurs along the line that is in the plane of the peptide group and at an angle of 34° with respect to the peptide C═O bond.[79,84] However, Krim et al. has shown that vibrations of adjacent amide chromophores are coupled and delocalized along the polypeptide backbone.[51,85] Furthermore, Asher and co-workers have experimentally demonstrated that the amide I vibrational mode exhibited noticeable interamide coupling in the α-helix conformation.[86,87] For this reason, it is more appropriate to consider the amide I Raman tensor for β-sheet and α-helix structures rather than that for the isolated peptide group. The largest principal axis for the β-sheet amide I Raman tensor is in the plane of the peptide bond and nearly parallel to the peptide carbonyls.[79,88] It has also been shown for the α-helix that the Raman tensor axis with the largest magnitude is parallel to the helix main axis, whereas the other two tensor axes are equivalent and perpendicular to the main axis.[79] Thus, the average and preferred angle distribution for β-sheet and α-helix amide I Raman tensors obtained from experimental results using the $N_{mp}(\theta)\sin(\theta)$ function represent the C═O orientation relative to the fibril axis.

The width of the orientation distribution function is used typically to estimate the uncertainty in determining the most probable orientation angle of a chemical group based on the polarized Raman spectroscopic measurements.[82] The half-height half-width of the orientation distribution function is about 15° for β-sheet and disulfide bonds in insulin fibrils (Figure 4). A higher orientation variability of C═O groups in α-helix, disordered and PPII structures results in a broader distribution (about 25°). In the case of a perfect alignment of fibrils in an anisotropic sample and a single orientation of chemical groups at a certain angle, the orientation distribution function is expected to be unimodal and given by the delta function centered at that angle. Several factors could result in broadening the orientation distribution function including an imperfect fibril alignment and multiple orientations of chemical groups with respect to the axis of the fibril. For example, the Eisenberg model predicts several different orientations of C═O groups in the insulin fibril core.[24] We used this prediction data to build a corresponding orientation distribution function assuming a perfect fibril alignment. The fact that there is an excellent agreement between this modeled distribution function and the function obtained experimentally (Figure 6A) indicates that the obtained broadening of the most probable orientation distribution function is indeed due to various orientations of carbonyl groups. In other words, the width of the orientation distribution function of C═O groups in the insulin fibril core is determined by the inhomogeneous broadening. The latter could be potentially tested by the site-specific isotope substitution of C═O groups and obtaining the orientation distribution functions for uniquely oriented labeled groups.

To evaluate the orientation of C═O groups for disordered portions of fibrils, we used the Raman tensor for the amide I mode proposed by Tsuboi and colleagues by investigating the Raman spectra of a uniaxial tetragonal aspartame.[89] As mentioned previously, the angle of 34° has been reported between this tensor and the peptide C═O bond for the isolated amide chromophore.[79,84] Once the angle between the carbonyl group and the PART is known, the orientation order parameters for the C═O bonds, $\langle P_2\rangle^{CO}$ and $\langle P_4\rangle^{CO}$, can be calculated from the experimentally determined $\langle P_2\rangle$ and $\langle P_4\rangle$ values using the Legendre addition theorem.[90]

Figure 6B shows the most probable orientation distribution function of C═O groups in the disordered parts of an insulin fibril (Figure 6B, red curve) calculated based on $\langle P_2\rangle^{CO}$ and $\langle P_4\rangle^{CO}$. The function shows a binormal distribution for the C═O group orientation with maxima at approximately 10° and 90°. This behavior can be explained assuming that at least two populations of disordered elements might co-occur within the fibril. These two populations consist of a similar number of groups and exhibit very different orientations, namely parallel and perpendicular to the fibril axis. As discussed in detail below, this behavior of carbonyl groups in the disordered portion of an insulin fibril qualitatively agrees with Eisenberg's model,[24] but quantitative comparisons result in several possible limitations. First, the 34° angle between the C═O group and the PART reported for an isolated peptide group might not be a good approximation for disordered peptide chains because of a possible vibrational coupling between adjacent peptide groups. Additionally, it has been shown that for a specific $\langle P_2\rangle$, there is a single most probable value of the order parameter $\langle P_4\rangle_{mp}$.[91] Therefore, the most probable value of the orientation order parameter $\langle P_4\rangle_{mp}^{CO}$ was approximated from the associated $\langle P_2\rangle^{CO}$.[92] In this case, the resultant most probable distribution function for the C═O had a single maximum at approximately 34° and the average orientation angle of C═O was approximately 45° (data not shown). Consequently, the calculated most probable orientation distribution function of the C═O groups in disordered parts of the insulin fibril should be considered as tentative.

Orientation of Disulfide Bonds. The R_z and R_x ratios as well as the order parameters $\langle P_2\rangle$ and $\langle P_4\rangle$ for disulfide bonds (513 cm^{-1} Raman band) are presented in Table 1. The $N_{mp}(\theta)$ function is centered at $\theta = 0°$ (Figure 4A) and the maximum of the $N_{mp}(\theta)\sin(\theta)$ function is at $\theta = 12°$ (Figure 4B). The mean distribution yielded an average orientation angle of 24°. It is worth noting that these values are very close to those obtained for the β-sheet component of the amide I band. It has been shown previously that disulfide bonds remain intact and preserve their conformation during insulin fibrillation.[93] Assuming that the Raman cross-section of a disulfide bond is independent of the conformation ($\sigma_{(ggg)} = \sigma_{(ggt)}$), we conclude that the two disulfide bonds ([B] Cys7-[A] Cys7 and [B] Cys19-[A] Cys20) with *ggg* conformation are preferably orientated at approximately 12 ± 8° with respect to the fibril axis. It should be noted that the 530 cm^{-1} Raman band assigned to the [A] Cys11-[A] Cys6 disulfide bond with *ggt* conformation did not show a significant polarization dependence. This result suggests that these S−S groups either do not

DOI: 10.1021/jacs.5b07535
J. Am. Chem. Soc. 2015, 137, 11312−11320

have a preferred orientation or are oriented close to 90° relative to the main axis of the fibril.

Tyrosine Residues. Raman tensors for several vibrational modes of the tyrosine residue have been previously reported.[67,79] Each insulin monomer contains four tyrosine and three phenylalanine residues, which do not necessarily have the same orientation relative to the main fibril axis. Obtaining information regarding the orientation of the individual side chains would require site-specific labeling,[45] which we plan to accomplish in the future. However, the approach described by Tsuboi[29,94] allows for information regarding the average orientation of the phenolic ring relative to the fibril axis to be obtained. Using the polarized Raman intensity ratios (I_{ZZ}/I_{XX}) of the bands at 643, 830, and 1209 cm^{-1} and the known values of the corresponding Raman tensors,[67] the average orientation angle of the phenolic ring normal is 60 ± 10° relative to the fibril axis.

Comparison to Existing Structural Models of Insulin Fibrils. Despite the fact that polarized Raman spectroscopy does not reveal the atomic-level structure, the obtained orientations of the chemical groups provide significant structural constraints and allow for the verification of the fibril structural models proposed earlier. Our experimental data suggest different orientations of individual secondary structure elements, including β-sheets, α-helices and PPII/disordered structures as well disulfide bonds and aromatic amino acid side chains within the insulin fibrils. Dobson and colleagues[25] have proposed a hypothetical arrangement of the polypeptide chains in the insulin amyloid protofilament (Figure 5B) based on cryo-EM data. Their model is qualitative, i.e., it does not provide structural information with atomic-level resolution, but it suggests that each insulin molecule occupies two β-strand layers with the strands parallel to each other. One can imagine that due to specific retentions two interchain disulfide bonds should be oriented rather parallel than perpendicular to the fibril axis, even though, Jimenez et al. specifically stated that "orientations of the termini and disulfide bonds within the curved structure are arbitrary". We found a strong orientation of two interchain disulfide bonds ([B] Cys7-[A] Cys7 and [B] Cys19-[A] Cys20) along the main axis of the fibril that does not contradict the model.

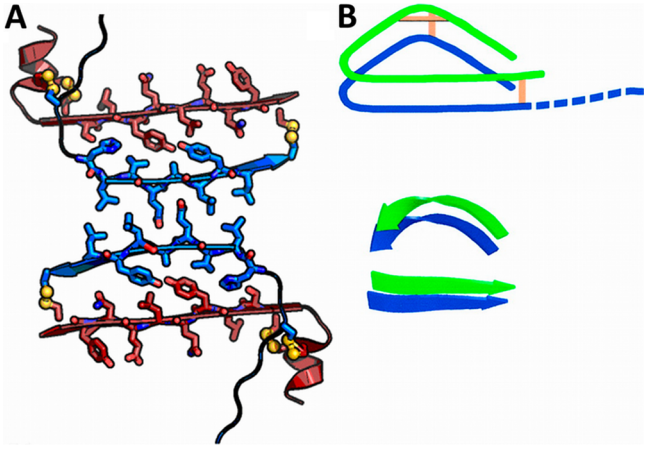

Figure 5. Structural models of the insulin fibril proposed by (A) Eisenberg and co-workers[24] and (B) Dobson and co-workers.[25] A model, built based on the structure of the LVEALYL peptide microcrystal as a template of the core of a full-length insulin fibril, offers the atomic-level resolution structure of the entire fibril and predicts the orientation and configuration of the disulfide bonds, β-strands, α-helices and disordered regions. B model, built based on Cryo-EM data, qualitatively predicts the orientation of β-strands and interchain disulfide bonds.

Eisenberg and co-workers have determined a limited set of possible arrangements of peptides in the cross-β structure, depending on the organization of the β-strands and β-sheets with respect to one another.[95] The insulin fibril model has been built based on the crystal structures of short amyloidogenic peptides LVEALYL and LYQLENY, which constitute the insulin fibril core.[24] These peptide sequences are found in the B and A chains of insulin, respectively. The proposed model predicts the structural organization of the entire insulin fibril (Figure 5A). We utilized the model to determine the orientation of disulfide bonds and the fibril core β-strands, α-helical and disordered parts, and compare the results to those of our polarized Raman spectroscopic study. Specifically, Figure 6 shows the comparison of the carbonyl group orientation in the fibril core (A) and disordered parts (B) of the fibril obtained from the polarized Raman spectroscopic data and that predicted by the model. The model-predicted angles are presented in the form of histograms and smooth Kernel functions (red curves). In the case of the fibril core (Figure 6A), the Kernel function showed a similar shape and close position (maximum at 14° and average at 18°) to those of the most probable distribution function (black curve, maximum at 12° and average at 24°) determined from the polarized Raman spectroscopic data. This result indicates an excellent agreement

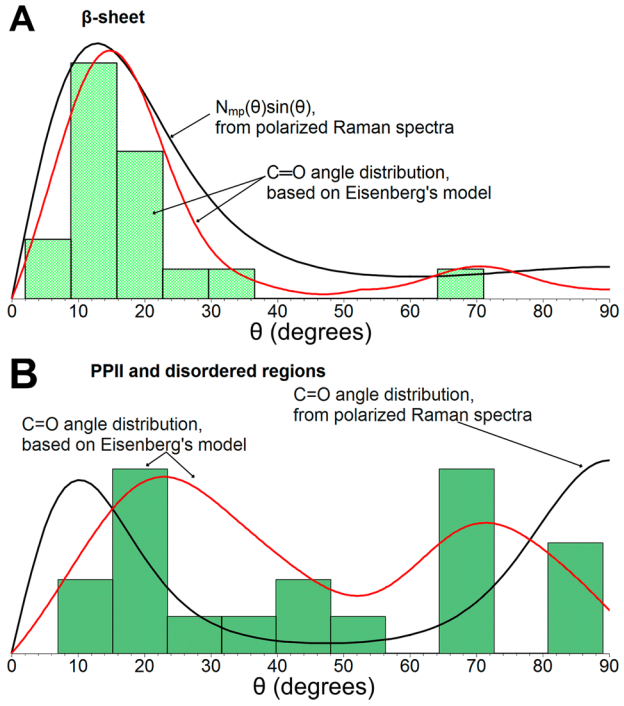

Figure 6. Orientation of C═O groups relative to the main fibril axis in the β-sheet core (A) and disordered parts (B) of human insulin fibrils: comparison of the polarized Raman spectroscopic data with those predicted by Eisenberg's model.[24] The orientation distribution functions obtained from the polarized Raman spectroscopic data (black curves). Histograms and smooth Kernel functions (red curves) represent the angle distribution predicted by the model. The data were normalized for comparison.

DOI: 10.1021/jacs.5b07535
J. Am. Chem. Soc. 2015, 137, 11312−11320

between the results of our polarized Raman spectroscopic study and Eisenberg's model in the case of the fibril core.

On the basis of Eisenberg's model, the angle distribution (red curve) of peptide carbonyls in the PPII and disordered regions with respect to the fibril axis has two maxima at approximately 25° and 72° according to the Kernel function shown in Figure 6B. The latter is in qualitative agreement with the most probable distribution function (black curve) for C═O groups calculated based on the polarized Raman measurements. A noticeable difference between the two distribution functions (red and black curves in Figure 6B) might result from a potential inaccuracy in calculating the angular distribution function for C═O groups based on the distribution function obtained for the corresponding PART as discussed above. Taking into account the composite contribution from disordered regions and PPII, we conclude that there is a qualitative agreement between the estimated distribution of the C═O group orientation based on polarized Raman measurements and that obtained from Eisenberg's model. The 1655 cm^{-1} amide I sub-band assigned to α-helical structures showed strong polarization dependence with the ZZ component being four times the XX component. This result indicates that the α-helices are well aligned and their orientation is close to the main axis of the fibril. In addition to this qualitative estimation, we calculated the average orientation angle for α-helix carbonyls relative to the fibril axis to be 33° based on the most probable distribution function. In contrast to our conclusion, Eisenberg's model predicts the average angle for α-helix C═O groups to be approximately 78°.

It is known that the frequency of the S−S stretching vibrational mode correlates with the internal rotation about the CS and CC bonds of the CCS-SCC moiety, which allows for differentiating the *ggg*, *ggt*, and *tgt* conformations based on Raman spectra.[72] The analysis of the S−S group orientation based on polarized Raman spectroscopy is simplified by the fact that the S−S stretching vibrational mode polarizability tensor is parallel to the S−S group. Our experimental data imply quite confidently that the two disulfide groups ([B] Cys7-[A] Cys7 and [B] Cys19-[A] Cys20) are parallel to each other and nearly parallel to the main fibril axis. The most probable angle between these two S−S groups and the fibril axis was estimated to be 12°. This conclusion disagrees with Eisenberg's model, which predicts that the two disulfide bonds, [B] Cys7-[A] Cys7 and [A] Cys6-[A] Cys11, are parallel to each other and oriented at approximately 72° with respect to the fibril axis. The third S−S bond, [B] Cys19-[A] Cys20, possesses an orientation at approximately 52°.

Our results clearly show that two interchain disulfide bonds are highly oriented relative to the fibril axis. Moreover, their orientation is parallel to the β-sheet component or, in other words, to the peptide carbonyl groups in the β-sheet (Figure 4). Such a strong and uniform orientation may indicate that these S−S groups are part of the fibril cross-β core. This observation is in agreement with our recent hydrogen−deuterium exchange data demonstrating that all of the disulfide bonds are located at the edge of the hydrophobic fibril core of insulin fibrils.[93] Furthermore, the tendency of Cys residues to participate in the formation of β-sheet areas on the surface of insulin fibrils was demonstrated with tip-enhanced Raman spectroscopy.[19]

Overall, the comparison of the orientation of carboxyl and disulfide groups evaluated on the basis of the polarized Raman spectroscopy of aligned insulin fibrils and predicted by Eisenberg's model showed excellent agreement for the fibril core carbonyls. At the same time, a significant difference was found for the orientation of α-helices and disulfide bonds. The model was built for the entire insulin fibril based mainly on the determined crystal structures of short amyloidogenic peptides LVEALYL and LYQLENY, which constitute the fibril core.[24] As a result, the fibril core structure was modeled accurately, whereas the remainder of the fibril, including disordered portions and α-helices, were not. We believe that polarized Raman spectroscopy of aligned fibrils provides additional structural constraints, which could allow for building a more accurate model of the entire fibril.

■ CONCLUSIONS

The conversion of proteins or peptides from their soluble functional states into structures referred to as amyloid fibrils is implicated in a large number of diseases. Atomic-level structural characterization of amyloid fibrils is challenging because of the limitations of solution NMR and X-ray crystallography when applied to insoluble, noncrystalline protein aggregates. Polarized Raman spectroscopy is uniquely suitable for probing amyloid fibrils, which can be aligned with high efficiency in an anisotropic sample. In this work, we demonstrated the great potential of polarized Raman spectroscopy for obtaining quantitative information regarding the organization of insulin fibrils. We specifically focused on determining the orientation of disulfide bonds, β-sheets, and α-helices relative to the fibril axis. Some degree of orientation of the disordered portions of the fibrils was also observed although the quantitative analysis of these data was challenging because of the uncertainty in determining an adequate polarizability tensor. In addition, the polarization effect was evident for aromatic amino acid residue side chains, but the averaging analysis was less informative in this case because of the variety of orientations of individual residues. The Raman scattering results allowed for the calculation of the order parameters $\langle P_2 \rangle$ and $\langle P_4 \rangle$ as well as the determination of the most probable orientation function for the disulfide bonds and each secondary structure element. The analysis of the obtained data indicated a high level of orientation of β-strands perpendicular to the long axis of the fibril and showed that the α-helical portions were also oriented, although to a lesser extent. We demonstrated that the two interchain disulfide bonds are an integral part of the fibril core with a preferred orientation distribution centered at an angle of approximately 12° to the fibril axis. The acquired data were compared with proposed structural models of insulin fibrils. The orientation of C═O groups in the core of insulin fibrils is centered at 12°, which is in excellent quantitative agreement with Eisenberg's model. At the same time, a significant difference was found for the orientation of α-helices and disulfide bonds. Two of the three insulin disulfide bonds were found to be oriented nearly parallel to the fibril axis as predicted by the qualitative Dobson model. Overall, the developed approach provides unique information regarding the orientation of certain chemical moieties in amyloid fibrils, which is not easily available from other structural methods, and offers additional constraints for building a structural model of the entire fibril.

■ EXPERIMENTAL SECTION

Insulin Fibril Preparation and Orientation. Human recombinant insulin (I2643) was purchased from Sigma-Aldrich (St Louis, MO) and used without further purification. Solutions of proteins, prepared immediately before fibrillation, were prepared by dissolving

DOI: 10.1021/jacs.5b07535
J. Am. Chem. Soc. 2015, 137, 11312−11320

protein powder in 1 mL of H_2O to achieve a final concentration of 10 g/L. The pH of the solution was adjusted to 2.5 by the addition of HCl. The solution was incubated at 65 °C for 24 h without agitation. The prepared fibrils were washed with an acidic solution (HCl, pH 2.5) and centrifuged for 30 min at 12000 *g* at 25 °C. This washing-spinning-resuspension procedure was repeated three times. Fibrils were sonicated for 5 min and then resuspended in pure water (dilution factor of 1:100, v/v). Aliquots (5−20 μL) of the fibril suspensions were dropped onto aluminum foil and air-dried.

Briefly, a drop of diluted protein solution forms a so-called "coffee ring" while drying.[47,96] Liquid evaporation causes a net liquid flow producing a shear force that carries radially oriented fibrils toward the perimeter of the droplet. Due to the geometric constraints, fibrils moving close to the droplet periphery have to change their orientation and align along the perimeter of the droplet, parallel to the outer edge of the ring.[97] A detailed description of the sample preparation procedure and sample orientation characteristics is given in SI.

Polarized Raman Spectroscopy. Spectra were recorded in the backscattering geometry with a LabRam HR Evolution Raman microscope (Horiba Jobin Yvon). A 785 nm diode laser was focused on the sample with a 100x objective (0.9 NA-Olympus). A 785 nm laser was utilized for excitation with the power adjusted to approximately 10 mW. No damage or spectral modifications were observed in samples under these conditions. A half wave plate was used to select the polarization of the incident laser beam and a polarizer was used to select the X or Z component of the scattered beam. An optical scrambler was installed before the spectrometer entrance slit to eliminate the polarization dependence of the grating. For polarization measurements, the excitation laser was focused on the edge of a dried droplet. Polarized Raman spectra were recorded for different polarization geometries, XX, XZ, ZX and ZZ, where the Z direction corresponds to the long axis of the fibrils and the *Y*-axis corresponds to the propagation direction of the incident and scattered light. The depolarization ratio was determined with polarized measurements on isotropic human insulin films/powders.

Data Analysis. Data acquisition and processing were performed using LabSpec6 software (Horiba Jobin Yvon). The spectra were baseline corrected over the 300−1800 cm^{-1} spectral range using a polynomial baseline, followed by 7−11 points smoothing. From the intensity ratios, R_z and R_x, the order parameters, $\langle P_2 \rangle$ and $\langle P_4 \rangle$, and the most probable orientation distribution, $N_{mp}(\theta)$, were calculated by applying a method previously described.[35] The complete experiment has been repeated two times for newly prepared samples and intensity ratios, R_z and R_x, were reproduced with 97% accuracy. All calculations were performed in MATLAB (version R2104a).

■ ASSOCIATED CONTENT

Supporting Information

The Supporting Information is available free of charge on the ACS Publications website at DOI: 10.1021/jacs.5b07535.

Sample preparation, raw polarized Raman spectra and an additional description of the procedure for determining the orientation of chemical groups based on polarized Raman spectroscopy. (PDF)

■ AUTHOR INFORMATION

Corresponding Author

*ilednev@albany.edu

Notes

The authors declare no competing financial interest.

■ ACKNOWLEDGMENTS

We are grateful to Dr. Victor Shashilov for stimulating discussions. This work was supported by the National Institute on Aging, National Institutes of Health, Grant R01AG033719 (I.K.L.).

■ REFERENCES

(1) Chiti, F.; Dobson, C. M. *Annu. Rev. Biochem.* **2006**, *75*, 333.
(2) Kelly, J. W. *Curr. Opin. Struct. Biol.* **1998**, *8* (1), 101−106.
(3) Sipe, J. D.; Cohen, A. S. *Crit. Rev. Clin. Lab. Sci.* **1994**, *31* (4), 325−354.
(4) Kurouski, D.; Dukor; Rina, K.; Lu, X.; Nafie; Laurence, A.; Lednev; Igor, K. *Biophys. J.* **2012**, *103* (3), 522−531.
(5) Makin, O. S.; Serpell, L. C. *FEBS J.* **2005**, *272* (23), 5950−5961.
(6) Tycko, R. *Curr. Opin. Struct. Biol.* **2004**, *14* (1), 96−103.
(7) Nelson, R.; Sawaya, M. R.; Balbirnie, M.; Madsen, A. O.; Riekel, C.; Grothe, R.; Eisenberg, D. *Nature* **2005**, *435* (7043), 773−778.
(8) Tycko, R. *Annu. Rev. Phys. Chem.* **2011**, *62* (1), 279−299.
(9) Serpell, L. C.; Sunde, M.; Benson, M. D.; Tennent, G. A.; Pepys, M. B.; Fraser, P. E. *J. Mol. Biol.* **2000**, *300* (5), 1033−1039.
(10) Makin, O. S.; Atkins, E.; Sikorski, P.; Johansson, J.; Serpell, L. C. *Proc. Natl. Acad. Sci. U. S. A.* **2005**, *102* (2), 315−320.
(11) Margittai, M.; Langen, R. *Q. Rev. Biophys.* **2008**, *41* (3−4), 265−297.
(12) Hiramatsu, H.; Goto, Y.; Naiki, H.; Kitagawa, T. *J. Am. Chem. Soc.* **2004**, *126* (10), 3008−3009.
(13) Rodríguez-Pérez, J. C.; Hamley, I. W.; Squires, A. M. *Biomacromolecules* **2011**, *12* (5), 1810−1821.
(14) Rodriguez-Perez, J. C.; Hamley, I. W.; Gras, S. L.; Squires, A. M. *Chem. Commun.* **2012**, *48* (97), 11835−11837.
(15) Shashilov, V. A.; Sikirzhytski, V.; Popova, L. A.; Lednev, I. K. *Methods* **2010**, *52* (1), 23−37.
(16) Wang, L.; Middleton, C. T.; Singh, S.; Reddy, A. S.; Woys, A. M.; Strasfeld, D. B.; Marek, P.; Raleigh, D. P.; de Pablo, J. J.; Zanni, M. T.; Skinner, J. L. *J. Am. Chem. Soc.* **2011**, *133* (40), 16062−16071.
(17) Shim, S.-H.; Gupta, R.; Ling, Y. L.; Strasfeld, D. B.; Raleigh, D. P.; Zanni, M. T. *Proc. Natl. Acad. Sci. U. S. A.* **2009**, *106* (16), 6614−6619.
(18) Ma, S.; Cao, X.; Mak, M.; Sadik, A.; Walkner, C.; Freedman, T. B.; Lednev, I. K.; Dukor, R. K.; Nafie, L. A. *J. Am. Chem. Soc.* **2007**, *129* (41), 12364−12365.
(19) Kurouski, D.; Deckert-Gaudig, T.; Deckert, V.; Lednev, I. K. *J. Am. Chem. Soc.* **2012**, *134* (32), 13323−13329.
(20) Kurouski, D.; Deckert-Gaudig, T.; Deckert, V.; Lednev; Igor, K. *Biophys. J.* **2014**, *106* (1), 263−271.
(21) Petkova, A. T.; Ishii, Y.; Balbach, J. J.; Antzutkin, O. N.; Leapman, R. D.; Delaglio, F.; Tycko, R. *Proc. Natl. Acad. Sci. U. S. A.* **2002**, *99* (26), 16742−16747.
(22) Lu, J.-X.; Qiang, W.; Yau, W.-M.; Schwieters; Charles, D.; Meredith; Stephen, C.; Tycko, R. *Cell* **2013**, *154* (6), 1257−1268.
(23) Nelson, R.; Eisenberg, D. In *Advances in Protein Chemistry*; Andrey Kajava, J. M. S., David, A. D. P., Eds.; Academic Press: New York, 2006; Vol. *73*, pp 235−282.
(24) Ivanova, M. I.; Sievers, S. A.; Sawaya, M. R.; Wall, J. S.; Eisenberg, D. *Proc. Natl. Acad. Sci. U. S. A.* **2009**, *106* (45), 18990−18995.
(25) Jiménez, J. L.; Nettleton, E. J.; Bouchard, M.; Robinson, C. V.; Dobson, C. M.; Saibil, H. R. *Proc. Natl. Acad. Sci. U. S. A.* **2002**, *99* (14), 9196−9201.
(26) Choi, J. H.; May, B. C. H.; Wille, H.; Cohen, F. E. *Biophys. J.* **2009**, *97* (12), 3187−3195.
(27) Oladepo, S. A.; Xiong, K.; Hong, Z.; Asher, S. A.; Handen, J.; Lednev, I. K. *Chem. Rev.* **2012**, *112* (5), 2604−2628.
(28) Tsuboi, M.; Kubo, Y.; Akahane, K.; Benevides, J. M.; Thomas, G. J. *J. Raman Spectrosc.* **2006**, *37* (1−3), 240−247.
(29) Tsuboi, M.; Kubo, Y.; Ikeda, T.; Overman, S. A.; Osman, O.; Thomas, G. J. *Biochemistry* **2003**, *42* (4), 940−950.
(30) Overman, S. A.; Tsuboi, M.; Thomas, G. J., Jr *J. Mol. Biol.* **1996**, *259* (3), 331−336.
(31) Bower, D. I. *J. Polym. Sci., Polym. Phys. Ed.* **1972**, *10* (11), 2135−2153.
(32) Sourisseau, C. *Chem. Rev.* **2004**, *104* (9), 3851−3892.
(33) Labarthet, F. L.; Buffeteau, T.; Sourisseau, C. *Appl. Spectrosc.* **2000**, *54* (5), 699−705.

DOI: 10.1021/jacs.5b07535
J. Am. Chem. Soc. 2015, 137, 11312−11320

(34) Labarthet, F. L.; Bruneel, J.-L.; Buffeteau, T.; Sourisseau, C.; Huber, M. R.; Zilker, S. J.; Bieringer, T. *Phys. Chem. Chem. Phys.* **2000**, *2* (22), 5154−5167.
(35) Rousseau, M.-E.; Lefèvre, T.; Beaulieu, L.; Asakura, T.; Pézolet, M. *Biomacromolecules* **2004**, *5* (6), 2247−2257.
(36) Kowalska, P.; Cheeseman, J. R.; Razmkhah, K.; Green, B.; Nafie, L. A.; Rodger, A. *Anal. Chem.* **2011**, *84* (3), 1394−1401.
(37) Tanaka, M.; Young, R. J. *J. Mater. Sci.* **2006**, *41* (3), 963−991.
(38) Hamley, I. W.; Castelletto, V.; Moulton, C. M.; Rodríguez-Pérez, J.; Squires, A. M.; Eralp, T.; Held, G.; Hicks, M. R.; Rodger, A. *J. Phys. Chem. B* **2010**, *114* (24), 8244−8254.
(39) Hiramatsu, H.; Goto, Y.; Naiki, H.; Kitagawa, T. *J. Am. Chem. Soc.* **2005**, *127* (22), 7988−7989.
(40) Pottel, H.; Herreman, W.; van der Meer, B. W.; Ameloot, M. *Chem. Phys.* **1986**, *102* (1−2), 37−44.
(41) Lefèvre, T.; Paquet-Mercier, F.; Rioux-Dubé, J.-F.; Pézolet, M. *Biopolymers* **2012**, *97* (6), 322−336.
(42) Lefèvre, T.; Rousseau, M.-E.; Pézolet, M. *Biophys. J.* **2007**, *92* (8), 2885−2895.
(43) Matsuno, M.; Takeuchi, H.; Overman, S. A.; Thomas, G. J., Jr *Biophys. J.* **1998**, *74* (6), 3217−3225.
(44) Takeuchi, H.; Matsuno, M.; Overman, S. A.; Thomas, G. J. *J. Am. Chem. Soc.* **1996**, *118* (14), 3498−3507.
(45) Rodriguez-Perez, J. C.; Hamley, I. W.; Squires, A. M. *Phys. Chem. Chem. Phys.* **2013**, *15* (33), 13940−13950.
(46) Ortiz, C.; Zhang, D.; Xie, Y.; Davisson, V. J.; Ben-Amotz, D. *Anal. Biochem.* **2004**, *332* (2), 245−252.
(47) Zhang, D.; Xie, Y.; Mrozek, M. F.; Ortiz, C.; Davisson, V. J.; Ben-Amotz, D. *Anal. Chem.* **2003**, *75* (21), 5703−5709.
(48) Ortiz, C.; Zhang, D.; Xie, Y.; Ribbe, A. E.; Ben-Amotz, D. *Anal. Biochem.* **2006**, *353* (2), 157−166.
(49) Sereda, V.; Lednev, I. K. *J. Raman Spectrosc.* **2014**, *45* (8), 665−671.
(50) Huang, K.; Maiti, N. C.; Phillips, N. B.; Carey, P. R.; Weiss, M. A. *Biochemistry* **2006**, *45* (34), 10278−10293.
(51) Krimm, S.; Bandekar, J. In *Advances in Protein Chemistry*; Anfinsen, J. T. E., Frederic, M. R., Eds.; Academic Press: New York, 1986; Vol. *38*, pp 181−364.
(52) Qian, W.; Krimm, S. *Biopolymers* **1992**, *32* (4), 321−326.
(53) Frisk, S.; Ikeda, R. M.; Chase, D. B.; Rabolt, J. F. *Appl. Spectrosc.* **2004**, *58* (3), 279−286.
(54) Mirkin, N. G.; Krimm, S. *J. Am. Chem. Soc.* **1991**, *113* (26), 9742−9747.
(55) Chen, X. G.; Schweitzer-Stenner, R.; Krimm, S.; Mirkin, N. G.; Asher, S. A. *J. Am. Chem. Soc.* **1994**, *116* (24), 11141−11142.
(56) Chen, X. G.; Schweitzer-Stenner, R.; Asher, S. A.; Mirkin, N. G.; Krimm, S. *J. Phys. Chem.* **1995**, *99* (10), 3074−3083.
(57) Schweitzer-Stenner, R.; Sieler, G.; Mirkin, N. G.; Krimm, S. *J. Phys. Chem. A* **1998**, *102* (1), 118−127.
(58) Dong, J.; Wan, Z.; Popov, M.; Carey, P. R.; Weiss, M. A. *J. Mol. Biol.* **2003**, *330* (2), 431−442.
(59) Ortiz, C.; Zhang, D.; Ribbe, A. E.; Xie, Y.; Ben-Amotz, D. *Biophys. Chem.* **2007**, *128* (2−3), 150−155.
(60) Serpell, L. C. *Biochim. Biophys. Acta, Mol. Basis Dis.* **2000**, *1502* (1), 16−30.
(61) Bouchard, M.; Zurdo, J.; Nettleton, E. J.; Dobson, C. M.; Robinson, C. V. *Protein Sci.* **2000**, *9* (10), 1960−1967.
(62) Deckert-Gaudig, T.; Deckert, V. *Phys. Chem. Chem. Phys.* **2010**, *12* (38), 12040−12049.
(63) Amenabar, I.; Poly, S.; Nuansing, W.; Hubrich, E. H.; Govyadinov, A. A.; Huth, F.; Krutokhvostov, R.; Zhang, L.; Knez, M.; Heberle, J.; Bittner, A. M.; Hillenbrand, R. *Nat. Commun.* **2013**, *4*, 2890.
(64) Lednev, I. K. *Biophys. J.* **2014**, *106* (7), 1433−1435.
(65) Chen, M. C.; Lord, R. C. *J. Am. Chem. Soc.* **1974**, *96* (15), 4750−4752.
(66) Williams, R. W.; Dunker, A. K. *J. Mol. Biol.* **1981**, *152* (4), 783−813.
(67) Tsuboi, M.; Ezaki, Y.; Aida, M.; Suzuki, M.; Yimit, A.; Ushizawa, K.; Ueda, T. *Biospectroscopy* **1998**, *4* (1), 61−71.
(68) Mangialardo, S.; Piccirilli, F.; Perucchi, A.; Dore, P.; Postorino, P. *J. Raman Spectrosc.* **2012**, *43* (6), 692−700.
(69) Van Wart, H. E.; Scheraga, H. A. *J. Phys. Chem.* **1976**, *80* (16), 1823−1832.
(70) Van Wart, H. E.; Lewis, A.; Scheraga, H. A.; Saeva, F. D. *Proc. Natl. Acad. Sci. U. S. A.* **1973**, *70* (9), 2619−2623.
(71) Van Wart, H. E.; Scheraga, H. A. *J. Phys. Chem.* **1976**, *80* (16), 1812−1823.
(72) Tu, A. T. *Raman Spectroscopy in Biology: Principles and Applications*; Wiley: New York, 1982.
(73) Norrman, M.; Schluckebier, G. *BMC Struct. Biol.* **2007**, *7* (1), 83.
(74) Kudryavtsev, A. B.; Mirov, S. B.; DeLucas, L. J.; Nicolete, C.; Van Der Woerd, M.; Bray, T. L.; Basiev, T. T. *Acta Crystallogr., Sect. D: Biol. Crystallogr.* **1998**, *54* (6−2), 1216−1229.
(75) Johnson, C. R.; Asher, S. A. *J. Raman Spectrosc.* **1987**, *18* (5), 345−349.
(76) Gazit, E. *FASEB J.* **2002**, *16* (1), 77−83.
(77) Wen, Z.-Q. *J. Pharm. Sci.* **2007**, *96* (11), 2861−2878.
(78) Tsuboi, M.; Ueda, T.; Ushizawa, K. *J. Mol. Struct.* **1995**, *352*−*353* (0), 509−517.
(79) Tsuboi, M.; Benevides, J. M.; Thomas, J. G. *Proc. Jpn. Acad., Ser. B* **2009**, *85* (3), 83−97.
(80) Richard-Lacroix, M.; Pellerin, C. *Macromolecules* **2012**, *45* (4), 1946−1953.
(81) Church, J. S.; Poole, A. J.; Woodhead, A. L. *Vib. Spectrosc.* **2010**, *53* (1), 107−111.
(82) Raghavan, M.; Sahar, N. D.; Wilson, R. H.; Mycek, M.-A.; Pleshko, N.; Kohn, D. H.; Morris, M. D. *J. Biomed. Opt.* **2010**, *15* (3), 037001−037001.
(83) Fratzl, P.; Paris, O.; Klaushofer, K.; Landis, W. J. *J. Clin. Invest.* **1996**, *97* (2), 396−402.
(84) Pajcini, V.; Chen, X. G.; Bormett, R. W.; Geib, S. J.; Li, P.; Asher, S. A.; Lidiak, E. G. *J. Am. Chem. Soc.* **1996**, *118* (40), 9716−9726.
(85) Krimm, S.; Abe, Y. *Proc. Natl. Acad. Sci. U. S. A.* **1972**, *69* (10), 2788−2792.
(86) Mikhonin, A. V.; Asher, S. A. *J. Phys. Chem. B* **2005**, *109* (7), 3047−3052.
(87) Myshakina, N. S.; Asher, S. A. *J. Phys. Chem. B* **2007**, *111* (16), 4271−4279.
(88) Nguyen, K. T.; King, J. T.; Chen, Z. *J. Phys. Chem. B* **2010**, *114* (25), 8291−8300.
(89) Tsuboi, M.; Ikeda, T.; Ueda, T. *J. Raman Spectrosc.* **1991**, *22* (11), 619−626.
(90) Ikeda, R.; Chase, B.; Everall, N. J. In *Vibrational Spectroscopy of Polymers: Principles and Practice*; Everall, N. J, Chalmers, J. M., Griffiths, P. R., Eds.; John Wiley & Sons, Ltd.: Chichester, 2007; pp 283−303.
(91) Bower, D. I. *J. Polym. Sci., Polym. Phys. Ed.* **1981**, *19* (1), 93−107.
(92) Richard-Lacroix, M.; Pellerin, C. *Macromolecules* **2013**, *46* (14), 5561−5569.
(93) Kurouski, D.; Washington, J.; Ozbil, M.; Prabhakar, R.; Shekhtman, A.; Lednev, I. K. *PLoS One* **2012**, *7* (6), e36989.
(94) Tsuboi, M.; Ushizawa, K.; Nakamura, K.; Benevides, J. M.; Overman, S. A.; Thomas, G. J. *Biochemistry* **2001**, *40* (5), 1238−1247.
(95) Sawaya, M. R.; Sambashivan, S.; Nelson, R.; Ivanova, M. I.; Sievers, S. A.; Apostol, M. I.; Thompson, M. J.; Balbirnie, M.; Wiltzius, J. J. W.; McFarlane, H. T.; Madsen, A. O.; Riekel, C.; Eisenberg, D. *Nature* **2007**, *447* (7143), 453−457.
(96) Deegan, R. D.; Bakajin, O.; Dupont, T. F.; Huber, G.; Nagel, S. R.; Witten, T. A. *Nature* **1997**, *389* (6653), 827−829.
(97) Li, Q.; Zhu, Y. T.; Kinloch, I. A.; Windle, A. H. *J. Phys. Chem. B* **2006**, *110* (28), 13926−13930.

DOI: 10.1021/jacs.5b07535
J. Am. Chem. Soc. 2015, 137, 11312−11320